Energy 270 (2023) 126945

Contents lists available at ScienceDirect

Energy

journal homepage: www.elsevier.com/locate/energy

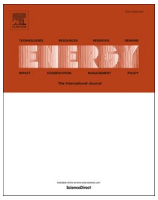

Day-ahead optimization dispatch strategy for large-scale battery energy storage considering multiple regulation and prediction failures

Mingze Zhang [a], Weidong Li [a,*], Samson Shenglong Yu [b], Kerui Wen [a], S.M. Muyeen [c]

[a] School of Electrical Engineering, Dalian University of Technology, Dalian, 116024, China
[b] School of Engineering, Deakin University, Melbourne, Victoria, 3216, Australia
[c] Department of Electrical Engineering, Qatar University, Doha, 2713, Qatar

ARTICLE INFO

Handling Editor: Henrik Lund

Keywords:
Large-scale battery energy storage
Active power regulation
Renewable energy system
Power dispatch
Day-ahead reserve

ABSTRACT

A large-scale battery energy storage station (LS-BESS) directly dispatched by grid operators has operational advantages of power-type and energy-type storages. It can help address the power and electricity energy imbalance problems caused by high-proportion wind power in the grid and ensure the secure, reliable, and economic operations of power systems together with conventional power generation units. To enable power systems to resist any power disturbance in the prediction failure set and cope with wind power and load fluctuations while meeting the load demand, a day-ahead dispatch optimization model to minimize operation costs on the dispatch day is established, which utilizes the regulation advantages of conventional units and a LS-BESS to participate in regulation services of diverse timescales and effectively achieve the coordination of various service demands. To account for wind power variations on the dispatch day, a robust optimization (RO) approach based on the budget uncertainty set is proposed, which improves the robustness and economy of grid operations against realistic uncertainties. The effectiveness of the day-ahead dispatch strategy is verified through extensive simulations and comparisons, which can better serve modern power systems with high penetration of wind power.

1. Introduction

With high penetrations of renewable energy, traditional homogeneous large-scale rotational generation units are being decommissioned. With this trend, power systems' inertia frequency response (IFR) [1,2], primary frequency response (PFR) [3,4], secondary frequency regulation (SFR) [5], and peak regulation (PR) [6] capabilities are becoming increasingly insufficient, and the active power balance and electricity energy at different timescales face great reliability challenges. BESSs have the advantages of rapid response, flexible electrical parameter adjustment, and bi-directional regulation [7], which can be used as a flexible resource to alleviate the problem associated active power balance in power systems [8]. To meet the dispatch and operation requirements in large power grids, the energy storage systems in the main grid are evolving toward large scale and large capacity [9]. At present, several pilot projects of energy storage at the hundred-megawatt level are being developed worldwide, such as the LS-BESS with rated power of 200 MW installed and put into operations in the city of Dalian, China. A grid-side LS-BESS can participate in multi-type active power regulation ancillary services [10] with conventional units under the unified dispatch of grid operators. This is considered an effective means to facilitate renewable energy integration, improve the flexibility and reliability of power supply, and ensure the security and stability operations of grids. It is necessary for grid operators to formulate the output and reserve scheduling of a LS-BESS and conventional units in the day-ahead stage, so that they can participate in active power regulation services in dispatch day operations. This motivates our research.

Authors in Refs. [8,9] proposed the configuration scheme of energy storage considering power system dispatch and operations, to guide the construction scale of energy storage. These are achieved by determining the demand capacity participating in active power regulations. Different from the propositions in Refs. [8,9], this study designs a day-ahead dispatch scheme from the perspective of grid operators based on the existing LS-BESS resource to realize the optimal daily active power operations of power systems. The participation of a LS-BESS in the day-ahead dispatch needs to consider the control strategy of an energy storage participating in active power regulation services, the cooperative operation mode between an energy storage and conventional units, and the treatment methods of wind power output uncertainties.

* Corresponding author.
E-mail address: wdli@dlut.edu.cn (W. Li).

https://doi.org/10.1016/j.energy.2023.126945
Received 15 November 2022; Received in revised form 9 February 2023; Accepted 11 February 2023
Available online 13 February 2023

Nomenclature

Y Number of regulation units in the power system that respond to step disturbances
M Number of conventional SFR units of the power system
$u_{i,t}$ A binary variable: "1" if regulation unit i is ON in time step t, and "0" otherwise.
v_t A binary variable: "1" if the LS-BESS is discharging in time step t, and "0" otherwise.
H_i Inertia time constant of regulation unit i (s)
$H_{S,t}$ Virtual inertial time constant of a LS-BESS in time step t (s)
$H_{sys,t}$ Inertia time constant of the power system in time step t (s)
$\Delta P_{L,t}$ Power deficit value of the power system in time step t (MW)
$K_{S,t}^{\mathrm{FFR}}$ Virtual inertial response coefficient of a LS-BESS in time step t (MWs/Hz)
$K_{S,t}^{\mathrm{PFR}}$ Virtual droop control coefficient of a LS-BESS to participate in PFR in time step t (MW/Hz)
$K_{G,t}^{\mathrm{PFR}}$ Droop control coefficient of conventional units to participate in PFR in time step t (MW/Hz)
$\Delta f^{\max}$ Maximum frequency deviation of conventional units for the droop relation (Hz)
$P_{G,t}^{\mathrm{PFR}}$ Capacity of conventional units to participate in PFR in time step t (MW)
$P_{G,i,t}$ Power output scheduling of conventional unit i in time step t (MW)
$P_{G,i}^{\max}$, $P_{G,i}^{\min}$ Maximum and minimum power outputs of conventional unit i (MW)
$\mathrm{T}_i^{\mathrm{on}}$, $\mathrm{T}_i^{\mathrm{off}}$ Minimum-up and minimum-down time of conventional unit i (h)
$R_{G,i}^{+}$, $R_{G,i}^{-}$ Maximum ramp-up and ramp-down limits in a time step of conventional unit i (MW)
$\omega_{j,t}$, ε_t Commitment factors of SFR unit j and a LS-BESS participating in SFR in time step t
$P_{G,t}^{\mathrm{SFR,up}}$, $P_{G,t}^{\mathrm{SFR,down}}$ Reserved upper and lower SFR spaces of conventional units to participate in SFR in time step t (MW)
$P_{S,t}^{\mathrm{FFR}}$, $P_{S,t}^{\mathrm{PFR}}$ Reserved spaces for a LS-BESS participation in FFR and PFR in time step t (MW)
$P_{S,t}^{\mathrm{SFR,up}}$, $P_{S,t}^{\mathrm{SFR,down}}$ Reserved upper and lower SFR spaces of a LS-BESS to participate in SFR in time step t (MW)
$P_{S,t}^{\mathrm{ch}}$, $P_{S,t}^{\mathrm{dis}}$ Charging and discharging power scheduling of a LS-BESS in time step t (MW)
η_C, η_D Charging and discharging efficiency of the LS-BESS
$P_S^{\max}$ Rated power capacity of a LS-BESS (MW)
$E_{S,t}$ Energy capacity of the LS-BESS in time step t (MWh)
E_S^{rated} Rated energy capacity of the LS-BESS (MWh)
Δt^{FFR}, Δt^{PFR} Time set for the LS-BESS to participate in FFR and PFR (s)
SoC_S^{ini} SoC value of the LS-BESS in the initial time step on the dispatch day
$SoC_S^{\max}$, $SoC_S^{\min}$ Upper and lower thresholds of the SoC value of the LS-BESS
$\Delta E_{S,t}^{\mathrm{FFR}}$, $\Delta E_{S,t}^{\mathrm{PFR}}$ Energy consumptions of the LS-BESS participating in FFR and PFR in time step t (MWh)
$\Delta E_{S,t}^{'}$ Energy consumptions of the LS-BESS in time step t (MWh)
$\Delta E_{S,t}^{\mathrm{SFR}}$, $\Delta E_{S,t}$ Energy consumptions of the LS-BESS participating in SFR and PR in time step t (MWh)
$P_{W,t}^{\mathrm{sup}}$, $P_{W,t}^{\mathrm{inf}}$ Upper and lower thresholds of wind power output in time step t (MW)
$C_{G,t}$, $C_{S,t}$ Operation costs of conventional units and a LS-BESS in time step t ($)
$C_{W,t}^{\mathrm{cur}}$ Wind power curtailment cost in time step t ($)
$P_{LD,t}$ Load demand of the power system in time step t (MW)

Relevant studies have been conducted in these aspects.

Regarding the operational strategy of a BESS participating in multi-type active power regulation services, some studies attempt to maximize economic benefits through refined management of state of charge (SoC) of the BESS. For example, authors in Ref. [11] took a BESS as a price maker to participate in the energy, reserve, and SFR markets, and proposed a bi-level bidding optimization framework that can obtain the optimal market clearing scheduling to maximize its revenue. Authors in Ref. [12] proposed an intra-day lookahead operation model for a behind-the-meter BESS to maximize its economic benefits through charging, discharging, and PFR behavior. Authors in Refs. [13,14] respectively established a two-stage bidding decision model and a bidding scheduling robust model to maximize their profits of an energy storage agent and an aggregated energy storages and wind resources participating in the joint energy and reserve markets. These studies belong to the autonomous regulation of a BESS based on the system frequency signal, which are generally applicable to a single energy storage [11,12] or an energy storage aggregator [13,14], rather than achieving the global optimization operations from the system perspective. In contrast, some studies on regulating a BESS to participate in active power regulations from the perspective of system operations generally consider certain types of services in daily operations, such as participation in PR and PFR [15,16], SFR [17], or absorption of renewable energy that is difficult to be accepted by power grids [18]. These studies do not consider a LS-BESS participation in power and electricity energy balance regulation services at various timescales in daily power system operations under the direct dispatch mode, which did not realize application values of a LS-BESS and could not enhance the security, reliability, and economy of power system operations.

Regarding the coordinated regulation strategy between a LS-BESS and conventional units, to take advantage of the rapid regulation speed of a BESS, researchers in Refs. [19,20] consider that the BESS releases a large amount of power immediately after the system is disturbed to directly compensate for the power deficit. Then its discharging power after the system's SFR response is gradually reduced. This has the problem of non-essential or excessive utilization of energy storage resources. For participating in SFR, some studies [21–23] consider filtering the regulation signal so that BESSs are responsible for high-frequency components and conventional units are responsible for low-frequency components, which makes BESSs in operations for a long time. In addition, the demand for high-frequency components is relatively small, BESSs may still have a large surplus space when the system has insufficient regulation capacity for low-frequency components, and therefore BESSs did not fully participate in the regulation. All the above shortcomings may restrict the advantages of BESSs in real power system operations.

Accounting for wind power uncertainties in each time step can make the dispatch decision more applicable in actual operations of power systems. For the treatment of uncertainties, some studies adopt the stochastic programming method based on some expectation scenarios [24,25], which clusters several typical scenarios for probability expectation value weighting. Some studies use the chance-constrained programming [26,27] to allow a certain degree of probabilistic deviations for constraints. All the above methods need to be based on a large

amount of probabilistic statistical or predictive information of wind power [28,29], which leads to the contradictions between the excessive number of selected scenarios and the accuracy and time consumption of the solution. To solve these problems, some researchers adopt the RO method [6,30,31] that does not need to account for too many scenarios to formulate the optimization operation strategy under the worst-case scenario, to achieve strong robustness of decisions. However, the occurrence probability of the worst-case scenario is low, and if the scenario is selected in each time step, the obtained results are more conservative, which does not benefit the system operation economy.

In summary, there are very few studies on the day-ahead dispatch strategy of a LS-BESS directly dispatched by grid operators to participate in active power regulation services at various timescales on a dispatch day in cooperation with conventional units. In view of this, this study proposes a day-ahead optimal dispatch framework that considers the participation of a LS-BESS in active power regulations of power systems from for the power system as a whole. The main contributions of this paper are listed as follows.

- To fully utilize the complementary operation advantages among the regulation units, responsibility allocation strategies are proposed for two types of regulation units to coordinatively participate in the multi-type active power regulation services of the power system to be directly dispatched by the grid operator.
- To formulate the sequential decisions of the day-ahead reserved space for each unit to participate in various active power regulation services on the dispatch day, a day-ahead dispatch optimization model is established to ensure frequency reliability after the occurrence of any power disturbance in the prediction failure set, considering net load fluctuations and the risk of wind power curtailment.
- To address the over-conservativeness problem of standard RO when dealing with wind power uncertainties on the dispatch day, the proposed RO approach based on the budget uncertainty set limits the perturbation values of uncertainties. This allows grid operators to limit total fluctuations of wind power over a large timescale according to the dispatch requirements and their own risk preferences.

The rest of this paper is organized as follows. Section 2 proposes coordination principles for a LS-BESS and conventional units to participate in multi-type active power regulation services. Section 3 establishes the day-ahead dispatch optimization model. Section 4 describes the treatment method for wind power uncertainties. Section 5 provides simulation studies and data analysis. Finally, this paper concludes in Section 6.

2. Responsibility allocation strategy for a LS-BESS and conventional units

In this section, we propose the cooperative regulation principle of a LS-BESS and conventional units for the four active power regulation services of IFR, PFR, SFR, and PR.

2.1. IFR and fast frequency regulation (FFR)

When power deficit occurs, conventional units release their inherent inertia energy caused by rotors' rotation to provide the resistance ability of power systems upon the disturbances [2,4]. This process is called the IFR of conventional units, which generally lasts for 0–5 s and acts as a buffer for the system frequency drop. When the frequency drops to the deadband f^{db} set by conventional units, governors start to act with the frequency difference through the droop control. This is the PFR of units and generally lasts for 5–60 s. However, a LS-BESS is connected to power grids through some power electronic devices, which cannot synchronize the frequency to participate in IFR and PFR. Therefore, it is necessary for a LS-BESS to achieve these regulations through FFR and virtual droop control.

Grid operators need to reserve sufficient inertia and PFR spaces for power systems in day-ahead scheduling to have the ability to withstand possible step disturbances on the dispatch day. In this paper, we reserve spaces for the most severe scenario in the prediction failure set to ensure that UFLS does not occur in the power grid after any disturbance occurs. Grid operators mainly focus on two frequency dynamic characteristic indexes [1]: the initial rate of change of frequency (RoCoF) $RoCoF^{0^+}$ and the frequency nadir f^{nadir} after the system is disturbed. After the most serious step disturbance occurs, the reserved space should ensure that $RoCoF^{0^+}$ does not exceed the allowable maximum limit $RoCoF^{\max}$ and f^{nadir} does not fall below the frequency critical value $f^{\min}$ of triggering UFLS. These frequency security constraints are formulated as,

$$RoCoF^{0^+} \le RoCoF^{\max} \tag{1a}$$

$$f^{\mathrm{nadir}} \ge f^{\min} \tag{1b}$$

Different from the participation of conventional units in IFR and PFR, a LS-BESS participates in FFR and PFR, which is paid by the grid operator. Therefore, grid operators should invoke a LS-BESS when regulation capacities of conventional units are insufficient, and thus, the timing of a LS-BESS participation in FFR and PFR can be determined.

Ignoring the load damping effect, the RoCoF of the power system is expressed as [4],

$$\Delta \dot{f}_t = \left(\Delta P_{G,t} + \Delta P_{S,t} - \Delta P_{L,t}\right) f_0 \,/\, \left(2 H_{sys,t} P_B\right) \tag{2}$$

where Δf_t is the frequency difference. Terms $\Delta P_{G,t}$ and $\Delta P_{S,t}$ are incremental power generations of conventional units and a LS-BESS in time step t, respectively, and f_0 is the initial frequency of the power system. Term P_B is the baseline power value of the system, and we set it as the sum of the rated power capacities of units that can participate in inertia regulation and PFR. $H_{sys,t}$ can be calculated as [32,33],

$$H_{\mathrm{sys},t} = \sum_{i=1}^{Y} \left(H_i u_{i,t} P_i^{\mathrm{N}} \,/\, P_B\right) \tag{3}$$

where term P_i^{N} is the rated power capacity of unit i.

According to (2), the value of $RoCoF^{0^+}$ after occurring disturbances in time step t can be described as,

$$\Delta \dot{f}_t\big|_{t=0^+} = RoCoF_t^{0^+} = \Delta P_{L,t} f_0 \,/\, \left(2 H_{\mathrm{sys},t} P_B\right) \tag{4}$$

In the day-ahead dispatch, it can be judged whether the $RoCoF^{0^+}$ value (i.e., $RoCoF_{nons,t}^{0^+}$) satisfies the security margin (as in (1a)) under the condition that a LS-BESS does not participate in FFR, based on the most serious fault $\Delta P_{L,t}^{\max}$. If so, the inertia time constant $H_{S,t}$ of the LS-BESS is set to 0, that is, it does not participate in FFR. Otherwise, a minimum value constraint on term $H_{\mathrm{sys},t}$ is assigned, as shown in (5). The related flowchart is shown in Fig. 1(a). Through the coordination between a LS-BESS and conventional units, the optimal value of $H_{S,t}$ can be determined after optimization.

$$H_{\mathrm{sys},t} \ge \Delta P_{L,t}^{\max} f_0 \,\Big/\, \left(2 RoCoF^{\max} P_B\right) \tag{5}$$

The reserved space for a LS-BESS participation in FFR can be calculated as,

$$P_{S,t}^{\mathrm{FFR}} = K_{S,t}^{\mathrm{FFR}} RoCoF^{\max} \tag{6}$$

where term $K_{S,t}^{\mathrm{FFR}}$ is written as,

$$K_{S,t}^{\mathrm{FFR}} = 2 H_{S,t} P_S^{\max} / f_0 \tag{7}$$

2.2. Primary frequency response

Conventional units respond linearly to changes of frequency differ-

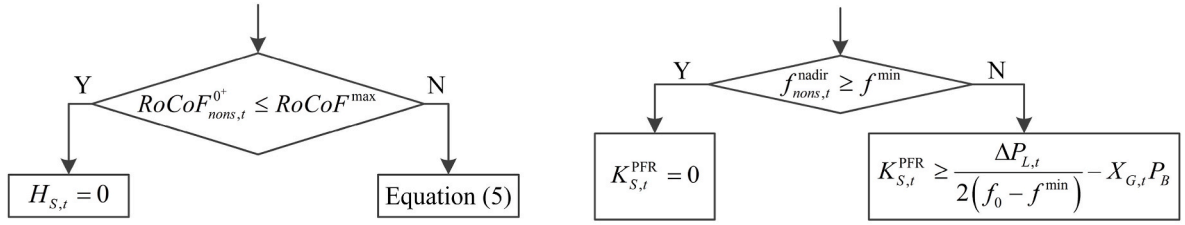

(a) Whether a LS-BESS participates in FFR (b) Whether a LS-BESS participates in PFR

Fig. 1. Schematic diagram of logic criteria for a LS-BESS participating in FFR and PFR.

ence through the droop characteristics, and their regulations to participate in PFR can be written as,

$$P_{G,t}^{\text{PFR}} = K_{G,t}^{\text{PFR}}\left(\Delta f^{\max} - f^{\text{db}}\right) \tag{8}$$

After the power system is disturbed, term f^{nadir} is calculated as,

$$f_t^{\text{nadir}} = f_0 - \frac{\Delta P_{L,t}}{2P_B\left(X_{G,t} + K_{S,t}^{\text{PFR}} \Big/ P_B\right)} \tag{9}$$

where $X_{G,t}$ is the sum of ramp gains of the whole online conventional units in time step t [34].

If the PFR capacities of conventional units are sufficient after the system is disturbed, the UFLS relay is not triggered because the f^{nadir} value (i.e., $f_{nons,t}^{\text{nadir}}$) satisfies the security margin (as in (1b)) under the condition that a LS-BESS does not participate in PFR, and the LS-BESS does not need to reserve PFR space. Otherwise, the reserved amount of a LS-BESS participating in PFR is obtained by (10). The related flowchart is shown in Fig. 1(b).

$$P_{S,t}^{\text{PFR}} = K_{S,t}^{\text{PFR}}\left(f_0 - f^{\min} - \Delta f^{\max}\right) \tag{10}$$

2.3. Secondary frequency regulation

SFR generally lasts for 30 s–15 min and can cope with wind power and load fluctuations within a dispatch time step. This regulation service is realized by grid operators sending dispatch instructions to regulation units through the required amount of power $P_{\text{req},t}^{\text{SFR}}$. In this paper, an affine allocation strategy is adopted and modified between conventional units and a LS-BESS, and the reserved SFR spaces are determined by optimizing the commitment factors. Taking reserved upper SFR space as an example, their expressions are shown as follows,

$$P_{G,t}^{\text{SFR,up}} = \sum_{j=1}^{M} \omega_{j,t} u_{j,t} P_{\text{req},t}^{\text{SFR,up}} \tag{11a}$$

$$P_{S,t}^{\text{SFR,up}} = \varepsilon_t P_{\text{req},t}^{\text{SFR,up}} \tag{11b}$$

$$\varepsilon_t + \sum_{j=1}^{M} \omega_{j,t} u_{j,t} = 1 \tag{11c}$$

2.4. Peak regulation

As an independent energy storage resource, a LS-BESS cooperatively operates with conventional units to meet the load demand in each time step and maximize the wind power acceptance on the basis of achieving the supply-demand balance of active power. The scenarios of high wind power and low load bring challenges for grid operators to make dispatch decisions. Generally, the anti-peak regulation characteristics of wind power described in Ref. [35] may make conventional units enter the deep peak regulation (DPR) state [36] and even require oil injection to support combustion, which seriously increases the system operation cost. In this situation, a LS-BESS can enhance the downward PR capability of power systems through its bi-directional regulation.

The PR costs of power systems include the power production and DPR costs of conventional units, as well as the operation cost of a LS-BESS. For grid operators, a trade-off should be made between reserved PR space and wind curtailment. More space can result in less curtailment or complete acceptance of wind power but will cause higher reserved cost. Conversely, less reserved space may lead to higher wind curtailment. Considering all these factors, the proposed optimization model is proposed and detailed below. The day-ahead dispatch optimization framework proposed in this paper is shown in Fig. 2.

3. Mathematical optimization model of day-ahead dispatch

Although a LS-BESS has the characteristics of power-type and energy-type energy storage, its dispatchable space is limited [18], so, it should make optimal coordination for the reserved spaces of the LS-BESS to participate in various types of active power regulation services. The goal of the day-ahead dispatch is to optimize the economy of power system operations. In this section, a day-ahead dispatch optimization model is established for conventional units and a LS-BESS to coordinatively participate in multi-type active power regulation services.

3.1. Objective function of the proposed dispatch model

In this paper, a dispatch day is divided into 96 timesteps, and each step Δt is 15 mins. In the day-ahead scheduling stage, grid operators make decisions on the reserved spaces for each regulation unit to participate in active power regulations in each time step, with minimizing the total operation cost C^{da} of the power system on a dispatch day. The objective function is expressed as,

$$\text{minimize } C^{\text{da}} = \sum_{t=1}^{96}\left(C_{G,t} + C_{S,t} + C_{W,t}^{\text{cur}}\right) \tag{12}$$

1) Conventional units: The decision variables related to conventional units include $u_{i,t}$, $P_{G,i,t}$, $P_{G,i,t}^{\text{SFR,up}}$, and $P_{G,i,t}^{\text{SFR,down}}$. Term $C_{G,t}$ can be calculated as,

$$C_{G,t} = \sum_{i=1}^{N}\left(C_{G,i,t}^{\text{b}} + C_{G,i,t}^{\text{e}} + C_{G,i,t}^{\text{op}} + C_{G,i,t}^{\text{SFR}} + C_{G,i,t}^{\text{DPR}}\right) \tag{13}$$

where

$$C_{G,i,t}^{\text{b}} = C_{G,i}^{\text{on}}\left(1 - u_{i,t-1}\right)u_{i,t} \tag{14a}$$

$$C_{G,i,t}^{\text{e}} = C_{G,i}^{\text{off}} u_{i,t-1}\left(1 - u_{i,t}\right) \tag{14b}$$

$$C_{G,i,t}^{\text{op}} = \left(a_i P_{G,i,t}^2 + b_i P_{G,i,t} + c_i u_{i,t}\right)\Delta t \tag{14c}$$

$$C_{G,i,t}^{\text{SFR}} = c_{G,i}^{\text{SFR}}\left(P_{G,i,t}^{\text{SFR,up}} + P_{G,i,t}^{\text{SFR,down}}\right)\Delta t \tag{14d}$$

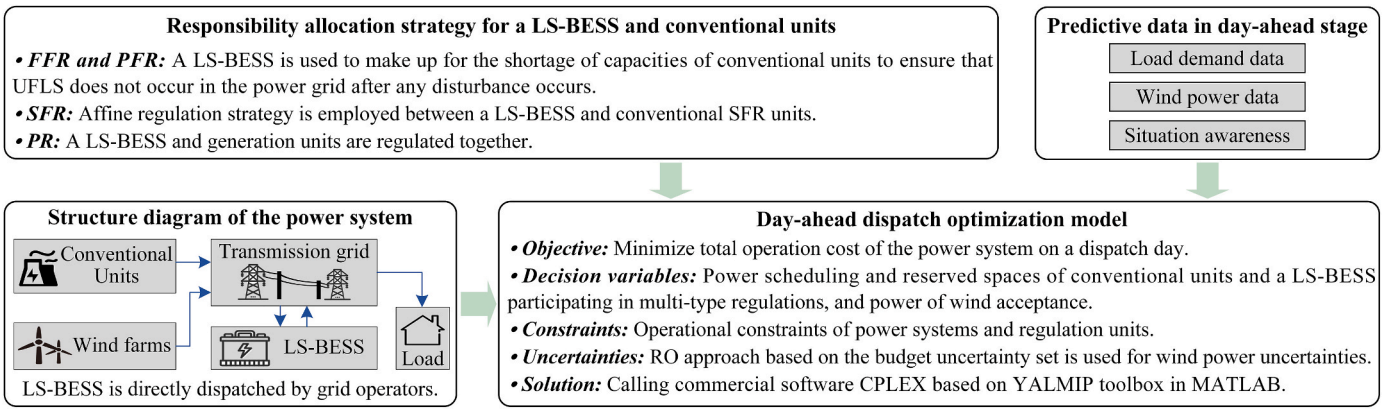

Fig. 2. The proposed day-ahead dispatch optimization framework for a LS-BESS participating in multiple active power regulation services.

$$C_{G,i,t}^{\mathrm{DPR}}=\begin{cases} c_G^{\mathrm{DPR1}}\left(P_{G,i}^{\mathrm{DPR1}}-P_{G,i,t}\right)\Delta t, P_{G,i}^{\mathrm{DPR2}}<P_{G,i,t}\le P_{G,i}^{\mathrm{DPR1}} \\ c_G^{\mathrm{DPR1}}\left(P_{G,i}^{\mathrm{DPR1}}-P_{G,i}^{\mathrm{DPR2}}\right)\Delta t+c_G^{\mathrm{DPR2}}\left(P_{G,i}^{\mathrm{DPR2}}-P_{G,i,t}\right)\Delta t, P_{G,i,t}\le P_{G,i}^{\mathrm{DPR2}} \end{cases} \tag{14e}$$

In (13), term N is the number of conventional units in the power system. The startup and shutdown costs $C_{G,i,t}^{\mathrm{b}}$ and $C_{G,i,t}^{\mathrm{c}}$ of conventional unit i in time step t are expressed by (14a) and (14b), they are related to the ON and OFF status of the unit during two consecutive steps. Equation (14c) describes the power production cost $C_{G,i,t}^{\mathrm{op}}$ of unit i in time step t, and a_i, b_i, and c_i are the production cost coefficients. Term $C_{G,i,t}^{\mathrm{SFR}}$ in (14d) represents the reserved SFR space cost of unit i in step t, and $c_{G,i}^{\mathrm{SFR}}$ is the unit electricity cost of participating in SFR. In (14e), term $C_{G,i,t}^{\mathrm{DPR}}$ represents the cost of conventional unit i participating in DPR in time step t. The participation of conventional units in PR can be divided into obligatory and paid regulations, and the DPR is a paid service. The cost calculation varies according to different regulation intervals, and in this paper, we consider dividing the DPR of conventional units into two intervals, i.e., $(P_{G,i}^{\mathrm{DPR2}}, P_{G,i}^{\mathrm{DPR1}}]$ and $[P_{G,i}^{\min}, P_{G,i}^{\mathrm{DPR2}}]$.

2) LS-BESS: The decision variables related to a LS-BESS include $P_{S,t}^{\mathrm{ch}}$, $P_{S,t}^{\mathrm{dis}}$, $P_{S,t}^{\mathrm{FFR}}$, $P_{S,t}^{\mathrm{PFR}}$, $P_{S,t}^{\mathrm{SFR,up}}$, and $P_{S,t}^{\mathrm{SFR,down}}$. Term $C_{S,t}$ is described by

$$C_{S,t}=C_{S,t}^{\mathrm{FFR}}+C_{S,t}^{\mathrm{PFR}}+C_{S,t}^{\mathrm{SFR}}+C_{S,t}^{\mathrm{op}} \tag{15}$$

where

$$C_{S,t}^{\mathrm{FFR}}=c_S^{\mathrm{FFR}}P_{S,t}^{\mathrm{FFR}}\Delta t \tag{16a}$$

$$C_{S,t}^{\mathrm{PFR}}=c_S^{\mathrm{PFR}}P_{S,t}^{\mathrm{PFR}}\Delta t \tag{16b}$$

$$C_{S,t}^{\mathrm{SFR}}=c_S^{\mathrm{SFR}}\left(P_{S,t}^{\mathrm{SFR,up}}+P_{S,t}^{\mathrm{SFR,down}}\right)\Delta t \tag{16c}$$

$$C_{S,t}^{\mathrm{op}}=c_S^{\mathrm{op}}\left(P_{S,t}^{\mathrm{ch}}+P_{S,t}^{\mathrm{dis}}\right)\Delta t \tag{16d}$$

In (15), terms $C_{S,t}^{\mathrm{FFR}}$, $C_{S,t}^{\mathrm{PFR}}$, and $C_{S,t}^{\mathrm{SFR}}$ are the reserved space costs of the LS-BESS participating in FFR, PFR, and SFR in time step t, respectively. $C_{S,t}^{\mathrm{op}}$ is the operation cost of the LS-BESS in step t. In (16a)–(16c), terms c_S^{FFR}, c_S^{PFR}, and c_S^{SFR} are unit electricity costs of the LS-BESS participating in FFR, PFR, and SFR, respectively, and c_S^{op} is the unit operation cost of the LS-BESS.

3) Wind power: The acceptance capacity is embodied in the mathematical model through term $C_{W,t}^{\mathrm{cur}}$, which can be expressed as,

$$C_{W,t}^{\mathrm{cur}}=c_W\left(P_{W,t}^{\mathrm{act}}-P_{W,t}\right)\Delta t \tag{17}$$

where term c_W is the unit cost of wind power curtailment, and $P_{W,t}$ is the wind power value accepted by grids in time step t. Term $P_{W,t}^{\mathrm{act}}$ is the actual wind power in step t, which is the uncertain factor, and its treatment method is described in Section 4.

3.2. Constraints of the proposed model

The day-ahead dispatch optimization model established from the perspective of power system operations should consider the relevant constraints of the system and regulation units. For the power system, it should meet the supply-demand balance of the active power under normal operations, as in (18a), and the total spinning reserve should meet the minimum requirement, as in (18b).

$$\sum_{i=1}^{N}P_{G,i,t}+P_{S,t}^{\mathrm{dis}}-P_{S,t}^{\mathrm{ch}}+P_{W,t}=P_{LD,t} \tag{18a}$$

$$\sum_{i=1}^{N}\left(u_{i,t}P_{G,i}^{\max}-P_{G,i,t}\right)+\left(P_S^{\max}-P_{S,t}^{\mathrm{dis}}+P_{S,t}^{\mathrm{ch}}\right)\ge\gamma P_{LD,t} \tag{18b}$$

where term γ is the minimum spinning reserve factor and is set to 8% in this study.

The regulation units should consider the various operation constraints of conventional units and a LS-BESS, such as power output limits, reserved capacity constraints, etc., which can be found in Appendix A. Other constraints of the proposed dispatch framework have been analyzed in Section 2.

4. Robust optimization model for wind power uncertainties

In this section, we establish a model to deal with wind power uncertainties through employing the RO approach based on the budget uncertainty set [30,37].

4.1. RO model establishment

To improve the over-conservativeness of the standard RO, we control the offset of uncertainties through increasing the 1-norm constraint on their perturbations to satisfy the uncertainty box set, that is, establishing the budget uncertainty set for wind power output. The above model can be expressed as,

$$P_{W,t}^{\mathrm{act}}=P_{W,t}^{\mathrm{pre}}+P_{W,t}^{\mathrm{unc}} \tag{19a}$$

$$P_{W,t}\le P_{W,t}^{\mathrm{act}} \tag{19b}$$

$$P_{W,t}^{\mathrm{act}}\in\left[P_{W,t}^{\mathrm{inf}}, P_{W,t}^{\mathrm{sup}}\right] \tag{19c}$$

$$P_{W,t}^{\mathrm{pre}} = \left(P_{W,t}^{\mathrm{sup}} + P_{W,t}^{\mathrm{inf}}\right) / 2 \tag{19d}$$

$$P_{W,t}^{\mathrm{unc}} = z_{W,t} P_{W,t}^{h} \tag{19e}$$

$$P_{W,t}^{h} = \left(P_{W,t}^{\mathrm{sup}} - P_{W,t}^{\mathrm{inf}}\right) / 2 \tag{19f}$$

$$\left|z_{W,t}\right| \le 1 \tag{19g}$$

$$\sum_{t=1}^{96} \left|z_{W,t}\right| \le \Gamma_W \tag{19h}$$

where $P_{W,t}^{\mathrm{pre}}$ is the prediction value of the wind power in time step t. $P_{W,t}^{\mathrm{unc}}$ is the prediction error, which raises the uncertainty. Term $P_{W,t}^{h}$ is the half-length value of wind power output interval, which characterizes the maximum offset of the actual value from the prediction value. The fluctuation range is enforced in (19g), where $z_{W,t}$ is the perturbation value of the uncertainty in time step t. Equation (19h) describes the budget constraint, where Γ_W is the budget value and can limit the total fluctuations of uncertainties.

The RO method is to obtain the optimal strategy for the worst-case scenario of uncertainties, and mapping this to our study is to formulate the day-ahead dispatch decision that minimizes the total operation cost of the power system when considering the maximum wind curtailment cost. Therefore, (17) can be further written as,

$$\sup \sum_{t=1}^{96} C_{W,t}^{\mathrm{cur}} = \sum_{t=1}^{96} c_W \left(P_{W,t}^{\mathrm{pre}} - P_{W,t}\right)\Delta t + \sup \sum_{t=1}^{96} c_W z_{W,t} P_{W,t}^{h} \Delta t \tag{20}$$

4.2. Model transformation

After adopting the RO approach based on the budget uncertainty set to deal with the wind power uncertainties, the objective function of the day-ahead dispatch optimization model becomes a double-layer nested problem in the form of "min-sup", and the decision variable of the inner optimization problem is the random variable of the outer problem. If the inner-layer "sup" problem is not transformed, the model is difficult to solve through existing techniques. Duality theory [38] is feasible for model transformation. Before applying it, (19b) needs to be transformed by

$$z_{W,t} \ge \left(P_{W,t} - P_{W,t}^{\mathrm{pre}}\right) \Big/ P_{W,t}^{h} \tag{21}$$

Constraints of the inner-layer optimization problem include (19g), (19h), and (21). Let $z_{W,t}^{+}$ and $z_{W,t}^{-}$ be orthogonal projections of $z_{W,t}$ and $-z_{W,t}$ on non-negative quadrants, respectively, that is,

$$z_{W,t}^{+} = \max\left\{z_{W,t}, 0\right\} \tag{22a}$$

$$z_{W,t}^{-} = \max\left\{-z_{W,t}, 0\right\} \tag{22b}$$

Therefore, we have

$$z_{W,t} = z_{W,t}^{+} - z_{W,t}^{-} \tag{23a}$$

$$\left|z_{W,t}\right| = z_{W,t}^{+} + z_{W,t}^{-} \tag{23b}$$

The inner-layer optimization problem can be described as,

$$\sup \sum_{t=1}^{96} \left[c_W P_{W,t}^{h} \left(z_{W,t}^{+} - z_{W,t}^{-}\right)\Delta t\right] \tag{24a}$$

$$\text{s.t.} \quad z_{W,t}^{+} + z_{W,t}^{-} \le 1 \tag{24b}$$

$$-z_{W,t}^{+} + z_{W,t}^{-} \le \left(P_{W,t}^{\mathrm{pre}} - P_{W,t}\right) \Big/ P_{W,t}^{h} \tag{24c}$$

$$\sum_{t=1}^{96} \left(z_{W,t}^{+} + z_{W,t}^{-}\right) \le \Gamma_W \tag{24d}$$

$$z_{W,t}^{+},\ z_{W,t}^{-} \ge 0 \tag{24e}$$

The optimization problem after the dual of the above equations are as follows,

$$\inf \left\{ \sum_{i=1}^{96} \left[\lambda^{(i)} + \sigma^{(i)} \left(P_{W,i}^{\mathrm{pre}} - P_{W,i}\right) \Big/ P_{W,i}^{h}\right] + \Gamma_W \delta \right\} \tag{25a}$$

$$\text{s.t.} \quad \lambda^{(i)} - \sigma^{(i)} + \delta \ge c_W P_{W,i}^{h} \Delta t \tag{25b}$$

$$\lambda^{(i)} + \sigma^{(i)} + \delta \ge -c_W P_{W,i}^{h} \Delta t \tag{25c}$$

$$\lambda^{(i)},\ \sigma^{(i)},\ \delta \ge 0 \tag{25d}$$

where terms $\lambda^{(i)}$, $\sigma^{(i)}$, and δ are the intermediate variables when solving the dual problem.

The objective function of the transformed model can be obtained by replacing the inner-layer problem described in (20) with (25a). The programming established in this paper can be solved through calling the commercial software CPLEX based on YALMIP toolbox in MATLAB.

5. Numerical results

The IEEE New England 10-unit 39-bus test system is used as a typical test system to verify the effectiveness of the proposed day-ahead dispatch scheme through numerical analyses.

5.1. Simulation settings

The following modifications are made to the case system: replacing units U5 and U6 with wind power of the total installed capacity of 950 MW and introducing a LS-BESS with rated capacity of 200 MW/800 MWh. The battery parameters are chosen based on the installed LS-BESS in the city of Dalian, China, which has rated power of 200 MW. The rated capacity (800 MWh) is calculated based on the grid code that peak regulation should operate at full power for at least 4 hours of continuous charging or discharging time [39]. In the conventional units, U2, U4, U7, and U8 are SFR units. The structure diagram of the modified power system is shown in Fig. 3. In addition, conventional units' parameters, load demand, and prediction value and maximum and minimum output curves of wind power are included in Appendix B.

We set $RoCoF^{\max} = 0.5$ Hz/s, $f_0 = 50$ Hz, $f^{\min} = 49.5$ Hz, and the most serious power deficit that may occur during each time step of the dispatch day is $10\%P_B$. For conventional units, terms f^{db} and $\Delta f^{\max}$ are set to 0.033 Hz and 0.2 Hz, respectively. In addition, we set $P_{G,i}^{\mathrm{DPR1}} = 50\%P_{G,i}^{\max}$, $P_{G,i}^{\mathrm{DPR2}} = 40\%P_{G,i}^{\max}$, $c_G^{\mathrm{DPR1}} = 60$ \$/MWh, and $c_G^{\mathrm{DPR2}} = 150$ \$/MWh. For the LS-BESS, we set $\eta_C = \eta_D = 95\%$, $SoC_S^{\mathrm{ini}} = 50\%$, and terms $SoC_S^{\max}$ and $SoC_S^{\min}$ are 90% and 10%, respectively. The operational parameter c_S^{op} is \$30/MWh, and c_S^{FFR} and c_S^{PFR} are \$60/MWh. The SFR requirement of the power system in each time step is taken as 5% of the load demand and 10% of the wind power prediction value [40,41], and the unit electricity price of regulation units participating in SFR is \$9/MWh. Term c_{W} is set to \$80/MWh, and Γ_{W} in the RO model is 32. The online conventional unit is U2 of the power system in the initial time step on the dispatch day.

5.2. Dispatch decisions and scheme comparisons

5.2.1. Situation settings and dispatch results

The established model is solved in 4500 seconds with the AMD Ryzen3 3200G with Radeon Vega Graphics 3.60 GHz processor. The

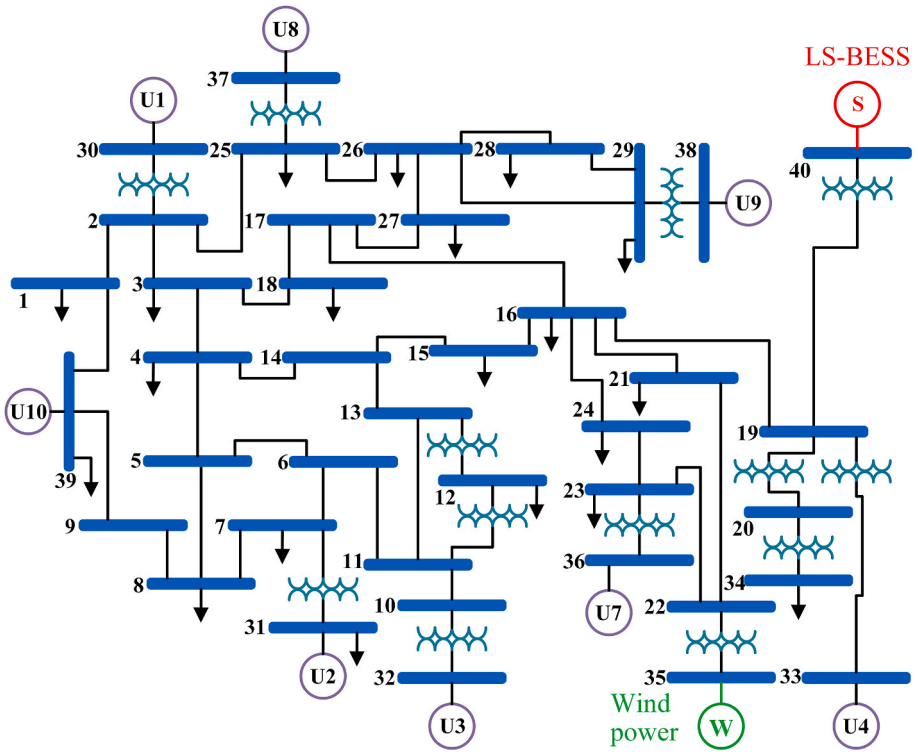

Fig. 3. Schematic diagram of the modified IEEE 10-unit 39-bus power system.

operation cost of the power system on the dispatch day is $621.90K, and the day-ahead reserved space scheduling of the LS-BESS and conventional units participating in multi-type active power regulation services are shown in Fig. 4. In addition, to illustrate the superiority of the proposed framework, we compare the day-ahead dispatch decisions obtained by our model and the following three situations.

- Situation 1: There is no LS-BESS, U5, or U6 in the power system. In this situation, the load exceeds the installed capacity of the system, and thus, the system cannot meet the load demand. Therefore, there is no feasible solution to the optimization model.
- Situation 2: There is no LS-BESS in the power system, but U5 and U6 are present. The corresponding optimization results in this situation are shown in Fig. 5, and the total operation cost of the power system is $683.33K.
- Situation 3: The LS-BESS only participates in FFR, PFR, and PR. The obtained decisions in this situation are shown in Fig. 6, and the total operation cost of the system is $690.03K.

5.2.2. Result analysis and discussions

1) FFR and PFR: It can be seen from Fig. 4(a) that the LS-BESS reserves FFR and PFR spaces to resist the possible step disturbances in 0–31 steps, which is caused by the insufficient response capability of conventional units in these periods. If the LS-BESS is not reserved for FFR and PFR spaces, when the most serious disturbance occurs, $RoCoF^{0^+}$ is 0.96 Hz/s and f^{nadir} drops to 49.03 Hz in 0–15 steps, two dynamic characteristic indexes of the system frequency are 0.89 Hz/s and 49.11 Hz in 16–19 steps, and 0.64 Hz/s and 49.34 Hz in 20–31 steps. UFLS will occur in these circumstances. When the 32nd step starts, U1 starts to operate, which increases the IFR and PFR regulation capacities of conventional units, and thus the LS-BESS does not need to reserve spaces for ensuring the frequency security.

According to the above analysis, if a LS-BESS is not available in the power system, the operation security cannot be satisfied when only U2 is online. Therefore, in Situation 2, we set the online units as U1 and U2 in the initial time step on the dispatch day. In Situation 2, although the frequency security of the power system can be ensured after large power deficit, it is necessary to increase the regulation capacity for step disturbances by putting larger capacity units into operations. Therefore, a LS-BESS can improve the operation economy while satisfying the power system security.

2) SFR: From the day-ahead dispatch strategies shown in Fig. 4, we can see that the conventional SFR units undertake fewer regulation tasks because of the LS-BESS's participation. Especially for U8, which is mainly dispatched to participate in PR rather than SFR. In the fast startup and shutdown units, U8 is dispatched to participate in the system operations preferentially over U9 and U10 because of its lower marginal power generation cost. The reserved SFR space cost of the LS-BESS accounts for 32.33% of its total operation cost on the dispatch day. In contrast, SFR units are regulated frequently to cope with net load fluctuations during the time step in Situation 2. In this situation, the scheduled power output of U2 cannot be reduced in 20–22 and 25–31 steps due to the reserved lower SFR space. To satisfy the supply-demand power balance, the scheduled output of U1 cannot be increased, which makes U1 enter the DPR state. U8 enters the DPR in the 22nd step as well. During 25–31 steps, U8 provides a lower SFR space under the critical power generation where it is about to enter the DPR state. For the power system considering a LS-BESS directly dispatched by grid operators, conventional units do not need to enter the DPR state in the case of reserving upper SFR spaces, and their power output reduction is not limited in the case of reserving lower SFR spaces, which can avoid other units from entering the DPR state. Therefore, a LS-BESS can improve the economy of the power system while ensuring the reliable operation.

Through comparing Figs. 4 and 6, since a LS-BESS does not reserve SFR space, the SFR units U8 and U7 are turned on successively during 0–16 steps in Situation 3, while only U2 is online in the proposed framework. The same is true after the 16th time step. In Situation 3, SFR units need to participate in regulations frequently. Compared with the LS-BESS participating in the whole timescale active power regulation services on the dispatch day, the reserved SFR cost of conventional SFR units under Situation 3 increases by 104.48%, and the total operation cost of the power system increases by 10.96%. In Situation 3, the LS-

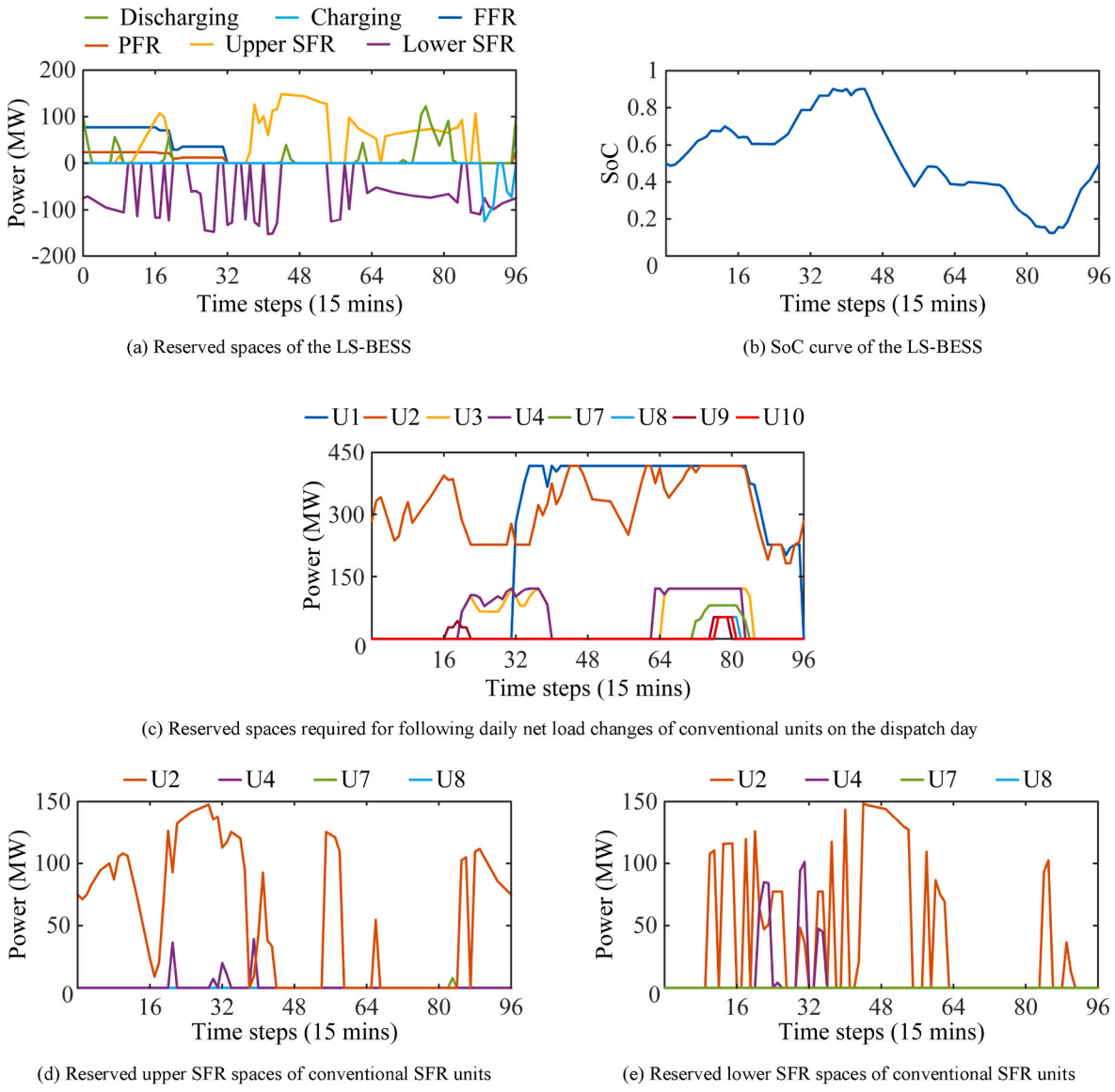

(a) Reserved spaces of the LS-BESS

(b) SoC curve of the LS-BESS

(c) Reserved spaces required for following daily net load changes of conventional units on the dispatch day

(d) Reserved upper SFR spaces of conventional SFR units

(e) Reserved lower SFR spaces of conventional SFR units

Fig. 4. Day-ahead dispatch decisions of the LS-BESS and conventional units in our proposed framework.

BESS is still reserved for FFR and PFR spaces in 0–31 steps. But the startup of SFR units improves the capacity of conventional units to cope with step disturbances, and thus the reserved FFR and PFR spaces of the LS-BESS becomes smaller. The reserved cost is reduced by 7.16%. The economic benefit of the LS-BESS under Situation 3 decreases by 33.64%. Therefore, the participation of a LS-BESS in active power regulation services on the whole dispatch day is more conducive to the economy of power systems than when it only participates in restricted types of services.

3) PR: A LS-BESS can discharge during the peak load periods, such as in 44–46 and 74–82 steps. It can also discharge to support the supply-demand power balance when the wind power and the total power output of conventional units are low, such as in 0–1, 7–8, and 61–62 steps. At the beginning of the 63rd step, grid operator dispatches U4 to participate in PR, and the LS-BESS exits. This is because the marginal power generation cost of U4 is about $16.82/MWh, which is significantly lower than the unit operation cost of the LS-BESS. During 89–95 steps, the load is low, but the wind power is high, so the LS-BESS keeps charging to increase the downward PR capacity of power systems, which promotes wind power acceptance. Meanwhile, the charging of LS-BESS can prevent conventional units from entering the DPR state. The DPR cost of conventional units under the proposed dispatch strategy is 0. But in Situation 2, the DPR costs of conventional units account for 6.71% of their total operation cost on the dispatch day.

In scenario 2, U1 is in the first gear of DPR except for the time steps of 32–87. In addition to the reason that SFR units needs to be reserved lower SFR spaces, grid operators allow conventional units to enter the first gear of DPR for accepting more wind power. The unit operation cost of conventional units in the first gear of DPR is less than the unit cost of wind power curtailment, so the power output of conventional units can be reduced to improve the acceptance value of wind power. However, the cost of conventional units under the second gear of DPR is very high, and if conventional units are dispatched to reduce their power output to the second gear of DPR to accept more wind power, it can lead to higher costs. Hence, wind power curtailment will be in place. Compared with Situation 2, a LS-BESS can reduce the installed capacity of conventional units in power systems and achieve the optimal economy while ensuring the security and reliability of grid operations.

5.3. *Sensitivity analysis of the budget parameters*

Fig. 7 shows the impact of varying Γ_W in {0, 8, 16, 24, …, 96} on the

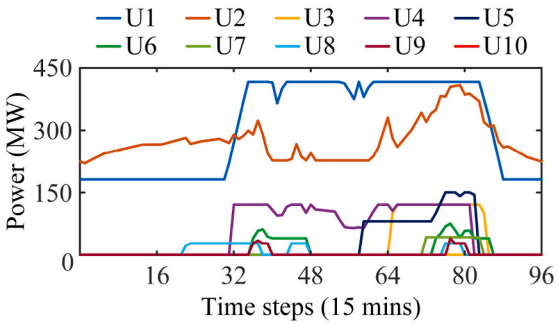

(a) Reserved spaces required for following daily net load changes of conventional units on the dispatch day

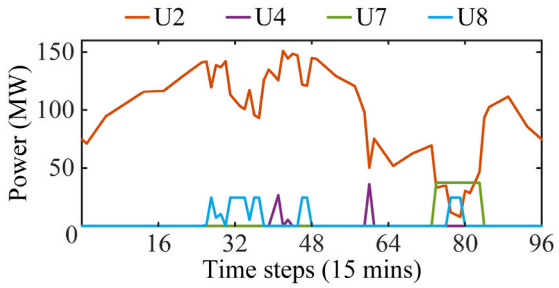

(b) Reserved upper SFR spaces of conventional SFR units

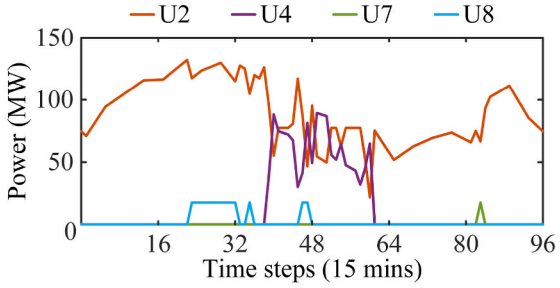

(c) Reserved lower SFR spaces of conventional SFR units

Fig. 5. Day-ahead power scheduling of conventional units in Situation 2.

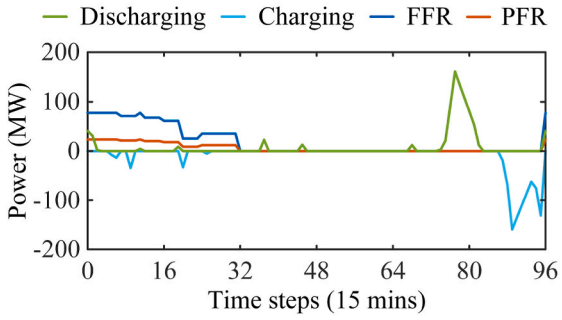

(a) Reserved spaces of the LS-BESS

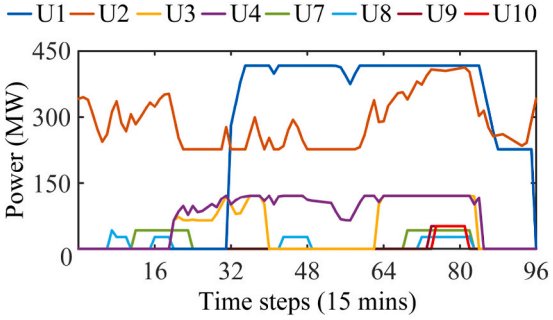

(b) Reserved spaces of units to follow daily net load changes

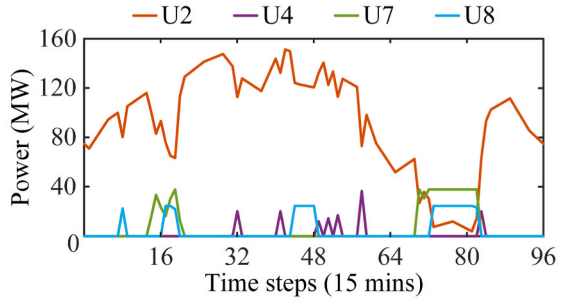

(c) Reserved upper SFR spaces of conventional SFR units

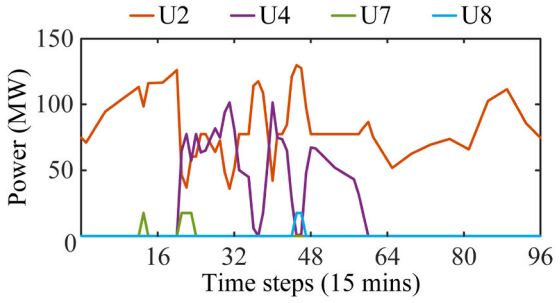

(d) Reserved lower SFR spaces of conventional SFR units

Fig. 6. Day-ahead scheduling of each regulation unit in Situation 3.

total operation cost of the power system on the dispatch day. The budget value has a greater impact on the total cost, which is caused by different degrees of uncertainties. The value of Γ_W can control the conservatism degree of the RO model based on the budget uncertainty set, and it reflects the requirement of grid operators for robust performance of decision results. When Γ_W is set to 0, grid operator does not consider the wind power uncertainty, and the actual output of the wind power on the dispatch day is considered the same as the day-ahead prediction value. In this case, the total dispatch cost is the minimum, but the obtained decisions do not have the robustness in the actual grid operations, and any change can lead to decision failure.

As Γ_W increases, the uncertainty degree of the actual wind power becomes larger, the obtained decisions tend to be more conservative, and the robust optimal solutions show worse economy as in Fig. 7. The

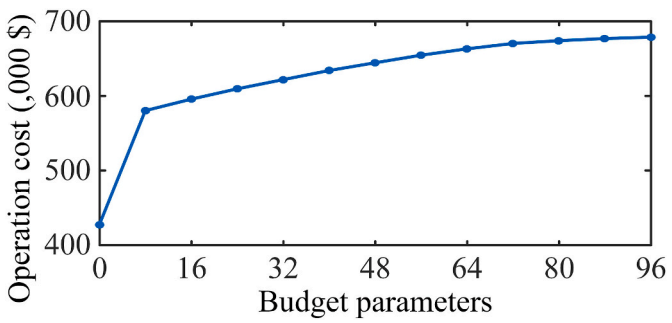

Fig. 7. Operation costs of the power system under different budget parameters.

total daily operation cost of the power system increases by 0.18% on average as the value of Γ_W increases by 1. When Γ_W is set to 96, the RO approach based on the budget uncertainty set reverts to a standard RO problem, which is equivalent to case where the perturbation value of actual wind power is unrestricted, and the range of uncertainties is a general box set. In this case, the robustness of the obtained decision is the highest, with the most conservativeness and worst economy. In practical power system dispatches, grid operators can select an appropriate budget parameter according to Fig. 7 and their preferences for robust performance of optimization results.

6. Conclusions

In this paper, we have established a day-ahead dispatch framework of a LS-BESS as an independent energy storage that cooperates with conventional units to participate in multi-type active power regulation services of power systems from the grid operation perspective, to ensure the security, reliability, and economy of grid active power operations. The numerical analysis and scenario comparisons of the modified IEEE 10-unit 39-bus power system result in the following conclusions.

- Compared to when a LS-BESS only participates in FFR, PFR, or RP, the economic benefit increases by 33.64% when the LS-BESS takes part in the entire time-scale active power regulation services on the dispatch day. At the same time, the total operation cost of the power system decreases by 10.96% with the LS-BESS. This indicates that a LS-BESS is more conducive to the economic operation of power systems through participating in all time-scale active power regulation services on the dispatch day.
- The service space for resisting step disturbances can be reserved according to the worst-case events in the prediction failure set, which can ensure the grid frequency security when the IFR and PFR capacities of conventional units are insufficient. The reserved space cost of a LS-BESS to cope with step disturbances on the dispatch day accounts for 52.38% of its total operation cost.
- A LS-BESS can coordinate with conventional SFR units to jointly reserve upper and lower SFR spaces in each dispatch time step. Compared to the traditional IEEE 10-unit 39-bus system, a LS-BESS can reduce the total operation cost of the power system by 8.99%.
- A LS-BESS can make the grid operate decommission some conventional units while having grid reliable operations. An appropriately scheduled LS-BESS can prevent some online units from entering the DPR state. A LS-BESS can achieve peak shaving through discharging and increase the downward PR capacity of power systems through charging to promote wind power acceptance.
- The proposed RO approach based on the budget uncertainty set for the uncertainties of the actual wind power output on the dispatch day considers the economy of power system operations while ensuring the robustness of dispatch decisions. Grid operators can weigh the conservativeness and economy of the dispatch strategy through adjusting the budget value parameter. The total operation cost of the power system increases by 0.18% when the budget value increases by 1.

Notwithstanding the merits of the proposed method, it also poses some limitations. In terms of regulation provision, we only consider LS-BESS as the regulation resources in this work, and the flexibility of power grid operations can be further enhanced by utilizing larger and diverse regulation resources, such as pumped-storage hydroelectric and demand-side distributed energy storage power stations. This fits well in our future research of devising a multi-regulation resource model in the power grid to work collaboratively with BESSs and conventional generators. Regarding the dispatch strategy, we did not consider multi-timescale scheduling of regulation resources, and conceptually a multi-timescale probabilistic dispatch framework can be established with a trade-off between the potential risk and reserved space, by measuring the extreme and low-probability disturbances. This could help achieve more secure, reliable, and economic power grid operations. For the model solution, the existing algorithm can be further improved to realize the fast solution of the practical power system operation schemes, with different solution accelerators. The above research aspects will be investigated in our future research, to diversify and strengthen the findings and solutions of this study.

Credit author statement

Mingze Zhang: Conceptualization, Methodology, Data curation, and Writing – original draft. **Weidong Li**: Supervision, Conceptualization, Project administration, and Writing – review & editing. **Samson Shenglong Yu**: Supervision, Visualization, Writing – review & editing, and Resources. **Kerui Wen**: Software, Investigation, and Validation. **S. M. Muyeen**: Formal analysis and Resources.

Declaration of competing interest

The authors declare that they have no known competing financial interests or personal relationships that could have appeared to influence the work reported in this paper.

Data availability

The authors are unable or have chosen not to specify which data has been used.

Acknowledgment

This work was supported by the National Natural Science Foundation of China [grant numbers U22A20223 and 51677018].

Appendix A

Operational constraints of conventional unit i are expressed as,

$$u_{i,t} - u_{i,t-1} - u_{i,\alpha} \le 0, \quad t \le \alpha \le \mathrm{T}_i^{\mathrm{on}} + t - 1 \tag{A1a}$$

$$u_{i,t-1} - u_{i,t} + u_{i,\beta} \le 1, \quad t \le \beta \le \mathrm{T}_i^{\mathrm{off}} + t - 1 \tag{A1b}$$

$$u_{i,t}P_{G,i}^{\min} \le P_{G,i,t} \le u_{i,t}P_{G,i}^{\max} \tag{A1c}$$

$$P_{G,i,t+1} - P_{G,i,t} \le R_{G,i}^{+}u_{i,t} + P_{G,i}^{\max}\left(1 - u_{i,t}\right) \tag{A1d}$$

$$P_{G,i,t} - P_{G,i,t+1} \le R_{G,i}^{-}u_{i,t+1} + P_{G,i}^{\max}\left(1 - u_{i,t+1}\right) \tag{A1e}$$

$$P_{G,i,t} - P_{G,i,t}^{\mathrm{SFR,down}} \ge u_{i,t}P_{G,i}^{\min} \tag{A1f}$$

$$P_{G,i,t} + P_{G,i,t}^{\mathrm{PFR}} + P_{G,i,t}^{\mathrm{SFR,up}} \le u_{i,t}P_{g,i}^{\max} \tag{A1g}$$

Equations (A.1a) and (A.1 b) represent the startup and shutdown constraints of conventional unit i, and the power output limits are enforced in (A.1c). The ramping constraints of unit i are shown in (A.1d) and (A.1e), and constraints (A.1f) and (A.1 g) are enforced for the reserved space of unit i.

Operational constraints of a LS-BESS on a dispatch day are described by

$$0 \le P_{S,t}^{\mathrm{dis}} \le P_{S}^{\max}v_t \tag{A2a}$$

$$0 \le P_{S,t}^{\mathrm{ch}} \le P_{S}^{\max}(1 - v_t) \tag{A2b}$$

$$0 \le P_{S,t}^{\mathrm{FFR}} + P_{S,t}^{\mathrm{PFR}} + P_{S,t}^{\mathrm{SFR,up}} \le P_{S}^{\max} - P_{S,t}^{\mathrm{dis}} + P_{S,t}^{\mathrm{ch}} \tag{A2c}$$

$$0 \le P_{S,t}^{\mathrm{SFR,down}} \le P_{S}^{\max} + P_{S,t}^{\mathrm{dis}} - P_{S,t}^{\mathrm{ch}} \tag{A2d}$$

$$\Delta E_{S,t} = P_{S,t}^{\mathrm{dis}} \Big/ \eta_D \Delta t - P_{S,t}^{\mathrm{ch}}\eta_C \Delta t \tag{A2e}$$

$$\Delta E_{S,t}^{\mathrm{FFR}} = P_{S,t}^{\mathrm{FFR}} \Big/ \eta_D \Delta t^{\mathrm{FFR}} \tag{A2f}$$

$$\Delta E_{S,t}^{\mathrm{PFR}} = P_{S,t}^{\mathrm{PFR}} \Big/ \eta_D \Delta t^{\mathrm{PFR}} \tag{A2g}$$

$$\Delta E_{S,t}^{\mathrm{SFR}} = P_{S,t}^{\mathrm{SFR,up}} \Big/ \eta_D \Delta t - P_{S,t}^{\mathrm{SFR,down}}\eta_C \Delta t \tag{A2h}$$

$$\Delta E_{S,t}^{'} = \Delta E_{S,t} + \Delta E_{S,t}^{\mathrm{FFR}} + \Delta E_{S,t}^{\mathrm{PFR}} + \Delta E_{S,t}^{\mathrm{SFR}} \tag{A2i}$$

$$E_{S,t+1} = E_{S,t} - \Delta E_{S,t}^{'} \tag{A2j}$$

$$E_{S,1} = E_{S,97} = SoC_{S}^{\mathrm{ini}}E_{S}^{\mathrm{rated}} \tag{A2k}$$

$$E_{S}^{\mathrm{rated}}SoC_{S}^{\min} \le E_{S,t} \le E_{S}^{\mathrm{rated}}SoC_{S}^{\max} \tag{A2l}$$

Constraints (A.2a) and (A.2b) represent the power output limits of a LS-BESS, and (A.2c) and (A.2d) are the reserved space constraints. The power-energy relationships of a LS-BESS are shown in (A.2e)–(A.2h). Constraint (A.2j) characterizes the step-coupling relationship, and (A.2k) is the daily operation cycle constraint of a LS-BESS. To prevent the over-charging and over-discharging of a LS-BESS, the SoC should be enforced within certain upper and lower thresholds, which leads to (A.2l).

Appendix B

Table B1
Parameters of conventional units.

Units	$C_{G,i}^{\mathrm{on}}$, $C_{G,i}^{\mathrm{off}}$ ($)	T_i^{on}, T_i^{off} (h)	a, b, c ($/MW^{2}h, $/MWh, $)	$P_{G,i}^{\max}$, $P_{G,i}^{\min}$ (MW)	$R_{G,i}^{+}$, $R_{G,i}^{-}$ (MW)	H_i (s)	$K_{i,t}^{\mathrm{PFR}}$ (p.u.)
U1	4500	8	0.00048, 16.19, 1000	455, 150	200	9.3	25
U2	5000	8	0.00031, 17.26, 970	455, 150	200	9.3	25
U3	550	5	0.00200, 16.60, 700	130, 20	80	8.1	20
U4	560	5	0.00211, 16.50, 680	130, 20	80	8.1	20
U7	260	3	0.00079, 27.74, 480	85, 25	80	5.8	17
U8	30	1	0.00413, 25.92, 660	55, 10	60	5.8	17
U9	30	1	0.00222, 27.27, 665	55, 10	60	5.8	17
U10	30	1	0.00173, 27.79, 670	55, 10	60	5.8	17

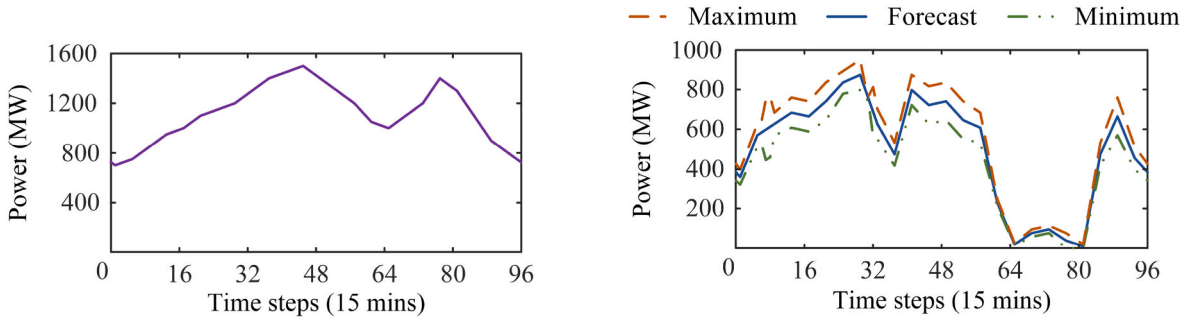

(a) Load demand (b) Wind power

Fig. B1. Relevant data of load and wind power in the test system.

References

[1] Yin Y, Liu T, Wu L, He C, Liu Y. Frequency-constrained multi-source power system scheduling against N-1 contingency and renewable uncertainty. Energy 2021;216:119296. https://doi.org/10.1016/j.energy.2020.119296.

[2] Cheng Y, Azizipanah-Abarghooee R, Azizi S, Ding L, Terzija V. Smart frequency control in low inertia energy systems based on frequency response techniques: a review. Appl Energy 2020;279:115798. https://doi.org/10.1016/j.apenergy.2020.115798.

[3] Debanjan M, Karuna K. An overview of renewable energy scenario in India and its impact on grid inertia and frequency response. Renew Sustain Energy Rev 2022;168:112842. https://doi.org/10.1016/j.rser.2022.112842.

[4] Dreidy M, Mokhlis H, Mekhilef S. Inertia response and frequency control techniques for renewable energy sources: a review. Renew Sustain Energy Rev 2017;69:144–55. https://doi.org/10.1016/j.rser.2016.11.170.

[5] Liu L, Hu Z, Duan X, Pathak N. Data-driven distributionally robust optimization for real-time economic dispatch considering secondary frequency regulation cost. IEEE Trans Power Syst 2021;36(5):4172–84. https://doi.org/10.1109/TPWRS.2021.3056390.

[6] Khojasteh M, Faria P, Vale Z. A robust model for aggregated bidding of energy storages and wind resources in the joint energy and reserve markets. Energy 2022;238:121735. https://doi.org/10.1016/j.energy.2021.121735.

[7] Yuan M, Sorknæs P, Lund H, Liang Y. The bidding strategies of large-scale battery storage in 100% renewable smart energy systems. Appl Energy 2022;326:119960. https://doi.org/10.1016/j.apenergy.2022.119960.

[8] Wang S, Li F, Zhang G, Yin C. Analysis of energy storage demand for peak shaving and frequency regulation of power systems with high penetration of renewable energy. Energy 2023;267:126586. https://doi.org/10.1016/j.energy.2022.126586.

[9] Chen X, Huang L, Liu J, Song D, Yang S. Peak shaving benefit assessment considering the joint operation of nuclear and battery energy storage power stations: hainan case study. Energy 2022;239:121897. https://doi.org/10.1016/j.energy.2021.121897.

[10] Mancarella P, Chicco G, Capuder T. Arbitrage opportunities for distributed multi-energy systems in providing power system ancillary services. Energy 2018;161:381–95. https://doi.org/10.1016/j.energy.2018.07.111.

[11] Khalilisenobari R, Wu M. Optimal participation of price-maker battery energy storage systems in energy and ancillary services markets considering degradation cost. Int J Electr Power Energy Syst 2022;138:107924. https://doi.org/10.1016/j.ijepes.2021.107924.

[12] Wen K, Li W, Yu SS, Li P, Shi P. Optimal intra-day operations of behind-the-meter battery storage for primary frequency regulation provision: a hybrid lookahead method. Energy 2022;247:123482. https://doi.org/10.1016/j.energy.2022.123482.

[13] Dimitriadis CN, Tsimopoulos EG, Georgiadis MC. Strategic bidding of an energy storage agent in a joint energy and reserve market under stochastic generation. Energy 2022;242:123026. https://doi.org/10.1016/j.energy.2021.123026.

[14] Khojasteh M, Faria P, Vale Z. A robust model for aggregated bidding of energy storages and wind resources in the joint energy and reserve markets. Energy 2022;238:121735. https://doi.org/10.1016/j.energy.2021.121735.

[15] Nasrolahpour E, Kazempour J, Zareipour H, Rosehart WD. A bilevel model for participation of a storage system in energy and reserve markets. IEEE Trans Sustain Energy 2018;9(2):582–98. https://doi.org/10.1109/TSTE.2017.2749434.

[16] Cao X, Zhao N. A cooperative management strategy for battery energy storage system providing enhanced frequency response. Energy Rep 2022;8:120–8. https://doi.org/10.1016/j.egyr.2021.11.092.

[17] Doenges K, Egido I, Sigrist L, Miguélez EL, Rouco L. Improving AGC performance in power systems with regulation response accuracy margins using battery energy storage system (BESS). IEEE Trans Power Syst 2020;35(4):2816–25. https://doi.org/10.1109/TPWRS.2019.2960450.

[18] Kwon K, Kim D. Enhanced method for considering energy storage systems as ancillary service resources in stochastic unit commitment. Energy 2020;213:118675. https://doi.org/10.1016/j.energy.2020.118675.

[19] Wen Y, Li W, Huang G, Liu X. Frequency dynamics constrained unit commitment with battery energy storage. IEEE Trans Power Syst 2016;31(6):5115–25. https://doi.org/10.1109/TPWRS.2016.2521882.

[20] Alcaide-Godinez I, Bai F, Saha TK, Castellanos R. Contingency reserve estimation of fast frequency response for battery energy storage system. Int J Electr Power Energy Syst 2022;143:108428. https://doi.org/10.1016/j.ijepes.2022.108428.

[21] Bai L, Li F, Hu Q, Cui H, Fang X. Application of battery-supercapacitor energy storage system for smoothing wind power output: an optimal coordinated control strategy. Proc IEEE Power Energy Soc General Meeting 2016:1–5. https://doi.org/10.1109/PESGM.2016.7741798.

[22] Sun Y, Tang X, Sun X, Jia D, Cao Z, Pan J, et al. Model predictive control and improved low-pass filtering strategies based on wind power fluctuation mitigation. J Mod Power Syst Clean Energy 2019;7:512–24. https://doi.org/10.1007/s40565-018-0474-5.

[23] Chong LW, Wong YW, Rajkumar RK, Isa D. An optimal control strategy for standalone PV system with battery-supercapacitor hybrid energy storage system. J Power Sources 2016;331:553–65. https://doi.org/10.1016/j.jpowsour.2016.09.061.

[24] Li J, Zhou J, Chen B. Review of wind power scenario generation methods for optimal operation of renewable energy systems. Appl Energy 2020;280:115992. https://doi.org/10.1016/j.apenergy.2020.115992.

[25] Noorollahi Y, Golshanfard A, Hashemi-Dezaki H. A scenario-based approach for optimal operation of energy hub under different schemes and structures. Energy 2022;251:123740. https://doi.org/10.1016/j.energy.2022.123740.

[26] Fallahi F, Bakir I, Yildirim M, Ye Z. A chance-constrained optimization framework for wind farms to manage fleet-level availability in condition based maintenance and operations. Renew Sustain Energy Rev 2022;168:112789. https://doi.org/10.1016/j.rser.2022.112789.

[27] Hosseini SA, Toubeau J-F, Grève ZD, Vallée F. An advanced day-ahead bidding strategy for wind power producers considering confidence level on the real-time reserve provision. Appl Energy 2020;280:115973. https://doi.org/10.1016/j.apenergy.2020.115973.

[28] Zakaria A, Ismail FB, Lipu MSH, Hannan MA. Uncertainty models for stochastic optimization in renewable energy applications. Renew Energy 2020;145:1543–71. https://doi.org/10.1016/j.renene.2019.07.081.

[29] Yan R, Wang J, Huo S, Qin Y, Zhang J, Tang S, et al. Flexibility improvement and stochastic multi-scenario hybrid optimization for an integrated energy system with high-proportion renewable energy. Energy 2023;263:125779. https://doi.org/10.1016/j.energy.2022.125779.

[30] Qiu H, Gu W, Liu P, Sun Q, Wu Z, Lu X. Application of two-stage robust optimization theory in power system scheduling under uncertainties: a review and perspective. Energy 2022;251:123942. https://doi.org/10.1016/j.energy.2022.123942.

[31] Gutierrez-Garcia F, Arcos-Vargas A, Gomez-Exposito A. Robustness of electricity systems with nearly 100% share of renewables: a worst-case study. Renew Sustain Energy Rev 2022;155:111932. https://doi.org/10.1016/j.rser.2021.111932.

[32] Fernández-Guillamón A, Muljadi E, Molina-García A. Frequency control studies: a review of power system, conventional and renewable generation unit modeling. Elec Power Syst Res 2022;211:108191. https://doi.org/10.1016/j.epsr.2022.108191.

[33] El-Bidairi KS, Nguyen HD, Mahmoud TS, Jayasinghe SDG, Guerrero JM. Optimal sizing of battery energy storage systems for dynamic frequency control in an islanded microgrid: a case study of Flinders Island, Australia. Energy 2020;195:117059. https://doi.org/10.1016/j.energy.2020.117059.

[34] Egido I, Fernandez-Bernal F, Centeno P, Rouco L. Maximum frequency deviation calculation in small isolated power systems. IEEE Trans Power Syst 2009;24(4):1731–8. https://doi.org/10.1109/TPWRS.2009.2030399.

[35] Hong Z, Wei Z, Li J, Han X. A novel capacity demand analysis method of energy storage system for peak shaving based on data-driven. J Energy Storage 2021;39:102617. https://doi.org/10.1016/j.est.2021.102617.
[36] Du M, Niu Y, Hu B, Zhou G, Luo H, Qi X. Frequency regulation analysis of modern power systems using start-stop peak shaving and deep peak shaving under different wind power penetrations. Int J Electr Power Energy Syst 2021;125:106501. https://doi.org/10.1016/j.ijepes.2020.106501.
[37] Bertsimas D, Sim M. The price of robustness. Oper Res 2004;52(1):35–53. https://doi.org/10.1287/opre.1030.0065.
[38] Bertsekas DP, Nedic A, Ozdaglar AE. Convex analysis and optimization. Belmont, MA, USA: Athena Sci; 2003, ISBN 1-886529-45-0.
[39] Northeast China Energy Regulatory Bureau of National Energy Administration. Operation rules of northeast electric power auxiliary service market. http://dbj.nea.gov.cn/dbjnea/zwfw/zcfg/E296CBF13C1746A5BC79E01393D6B718/index.shtml. [Accessed 8 February 2023].
[40] Wang X, Ying L, Lu S. Joint optimization model for primary and secondary frequency regulation considering dynamic frequency constraint. Power Syst Technol 2020;44(8):2858–67. https://doi.org/10.13335/j.1000-3673.pst.2019.1920.
[41] Zhang Y, Wang J, Wang X. Review on probabilistic forecasting of wind power generation. Renew Sustain Energy Rev 2014;32:255–70. https://doi.org/10.1016/j.rser.2014.01.033.